

This article was downloaded by:

On: 30 January 2011

Access details: *Access Details: Free Access*

Publisher *Taylor & Francis*

Informa Ltd Registered in England and Wales Registered Number: 1072954 Registered office: Mortimer House, 37-41 Mortimer Street, London W1T 3JH, UK



Separation & Purification Reviews

Publication details, including instructions for authors and subscription information:

<http://www.informaworld.com/smpp/title~content=t713597294>

Multicomponent Interference Phenomena in Ion Exchange Columns

Q. Yu^a; N. -H. L. Wang^a

^a School of Chemical Engineering, West Lafayette, Indiana

To cite this Article Yu, Q. and Wang, N. -H. L.(1986) 'Multicomponent Interference Phenomena in Ion Exchange Columns', Separation & Purification Reviews, 15: 2, 127 — 158

To link to this Article: DOI: 10.1080/03602548608058534

URL: <http://dx.doi.org/10.1080/03602548608058534>

PLEASE SCROLL DOWN FOR ARTICLE

Full terms and conditions of use: <http://www.informaworld.com/terms-and-conditions-of-access.pdf>

This article may be used for research, teaching and private study purposes. Any substantial or systematic reproduction, re-distribution, re-selling, loan or sub-licensing, systematic supply or distribution in any form to anyone is expressly forbidden.

The publisher does not give any warranty express or implied or make any representation that the contents will be complete or accurate or up to date. The accuracy of any instructions, formulae and drug doses should be independently verified with primary sources. The publisher shall not be liable for any loss, actions, claims, proceedings, demand or costs or damages whatsoever or howsoever caused arising directly or indirectly in connection with or arising out of the use of this material.

MULTICOMPONENT
INTERFERENCE PHENOMENA IN
ION EXCHANGE COLUMNS

Q. Yu and N.-H.L. Wang
School of Chemical Engineering
West Lafayette, Indiana 47907

ABSTRACT

Extensive computer simulations of multicomponent ion exchange processes in fixed beds are reported. The simulations are based on the local equilibrium theory developed by Helfferich and Klein. The simulations illustrate through computer graphics how the various ions separate and migrate in a column. Detailed concentration profiles as a function of time are shown for cyclic chromatographic operations such as elution, displacement, and selective displacement processes. The simulations elucidate the main features of the interference phenomena as a result of solute competition for the sorbent sites. These simulations also provide important guidelines for designing bulk separation processes, for example, the strategies of recovery, the choices of cyclic operations, feed size, presaturant, eluant, and displacer.

Correspondence: Dr. Nien-Hwa Linda Wang, School of Chemical Engineering, West Lafayette, IN 47907. Phone: (317)494-4065

I. INTRODUCTION

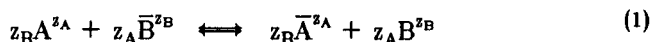
Chromatography is a highly selective separation technique which is widely used for analyzing complex mixtures. When chromatography is used for analysis, a very dilute sample is used to ensure negligible competition among various solutes. In such a dilute system, the chromatogram is straightforward and well understood^{1,2}. This method, however, is expensive and inefficient for large-scale bulk separations. In the conventional elution method, for example, a small feed pulse with low solute concentration is processed and only a small fraction of the total column capacity is used. When large feeds and high solute concentrations are used, the effects of solute competition (or interference) become important and result in complex solute distribution and migration within the column. The dynamics for concentrated systems are much less understood than those in dilute systems. The purpose of this paper is to elucidate the interference phenomena through detailed computer simulations of column dynamics. The understanding of this phenomena can provide valuable insights in designing columns for large-scale bulk separations.

Most chromatography theories in the literature are concerned with the dilute systems in which the interference is negligible. The most extensive discussion on the interference phenomena in ion exchange systems has been reported in the book by Helfferich and Klein³. A parallel treatise formulated for adsorption systems has also been reported by Rhee, Aris, and Amundson^{4,5,6}. No mass transfer effects were considered in these theories. These theories have been applied in analyzing the following systems: water treatment⁷, two-way chromatography⁸, dialysis fluid regeneration^{9,10}, displacement chromatography^{11,12}, and adsorption of chlorotoluene isomer mixtures¹³. All these experimental studies indicate that the main features of effluent histories can be well predicted by the local equilibrium theories. Mass transfer effects mainly reduce the slopes of the breakthrough curves and peak heights if the effects are pronounced.

In this paper, the local equilibrium theory developed by Helfferich and Klein is briefly summarized. Extensive computer simulation results for operations involving a single step change and multiple step changes are reported. The fundamental features of the interference phenomena are illustrated through the column dynamics. The implications on designing bulk separation processes are also discussed.

II. SUMMARY OF INTERFERENCE THEORY

The ion exchange of two ion species, A and B, in an ion exchanger can be described by the following reaction:



where z_A and z_B are the valence numbers of A and B. \bar{A} and \bar{B} represent ion species bound to the solid phase. An equilibrium constant K can be written for this process according to the mass action law:

$$K = \frac{\bar{a}_A^{z_B} \bar{a}_B^{z_A}}{a_A^{z_B} a_B^{z_A}} \quad (2)$$

Where a and \bar{a} are the activities in the mobile phase and in the stationary phase respectively. Since activities are usually difficult to measure, a binary selectivity coefficient K_{AB} is usually preferred for correlating the equilibrium data.

$$K_{AB} = \frac{\bar{c}_A^{z_B} \bar{c}_B^{z_A}}{c_A^{z_B} c_B^{z_A}} \quad (3)$$

where C_i and \bar{C}_i are the normalities of species i in the mobile phase and in the stationary phase respectively.

For systems involving only monovalent ions, the selectivity coefficient K_{AB} is the same as the separation factor α_{AB} , which is simply the distribution coefficient of species A divided by that of species B.

$$\alpha_{AB} \equiv \frac{\bar{c}_A/c_A}{\bar{c}_B/c_B} = \frac{y_A/x_A}{y_B/x_B} \quad (4)$$

where

$$x_A = c_A/c, \quad y_A = \bar{c}_A/\bar{c}; \quad (5)$$

c is the total ion concentration in the mobile phase; \bar{c} is the total ion concentration in the stationary phase; x_A and y_A are the normalized concentrations of species A in the mobile and stationary phases. The separation factor α_{AB} is a measure of the relative affinity of A against B. It is obvious that α_{AB} is not a true thermodynamic constant, especially for systems with ions of different valences. For many engineering applications, however, the separation factors are approximately constant because the changes in composition are small. We can rank all the species in a multicomponent system according to their separation factors. In this affinity sequence, Species 1 is the most preferred species and Species n is the least preferred. Therefore,

$$1 = \alpha_{11} < \alpha_{12} < \alpha_{13} \dots < \alpha_{1n} \quad (6)$$

In an ion exchange column, compositions of various ions are functions of both time and distance from the column inlet. At a given time, the composition is only a function of the distance. This is called a "column profile." At a given location, the composition is a function of time. This is called a "history". The histories at the column inlet and exit are called respectively the influent history and the effluent history.

In a column profile or history, the region of constant compositions are called concentration "plateaus". While the varying-composition regions that separate plateau zones are called "waves" or "boundaries". A wave is said to be "diffuse" if the variation is gradual, and "sharp" if the variation is abrupt.

A change in the input composition will generate a set of waves which propagate through the column at different speeds. The concentration velocity u_{c_i} of a given concentration value c_i is given by the expression

$$u_{c_i} \equiv \left[\frac{\partial z}{\partial t} \right]_{c_i} \quad (7)$$

The concentration velocity may refer to the concentration in the mobile phase, in the stationary phase or in both phases.

An "adjusted time" τ is used in order to simplify the expression for wave speeds. τ is defined as follows:

$$\tau \equiv \frac{Cu_0}{\bar{C}} [t - z/u_0] \quad (8)$$

where C and \bar{C} are the total ion concentrations per unit bed volume in the mobile phase and in the stationary phase respectively, and u_0 is the interstitial velocity. The adjusted time τ has the dimension of length. A dimensionless time T can be defined as τ divided by column length L .

$$T \equiv \tau/L \quad (9)$$

T represents the amount of solute input to the column during $T = 0$ and T divided by the total column capacity. Therefore, T is a measure of column loading. At $T = 1$, the column loading is 100%. A dimensionless distance Z^* can be defined as $Z^* = z/L$. An adjusted velocity for a concentration wave μ_{c_i} or μ_{x_i} can be defined in terms of the adjusted time τ .

$$\mu_{c_i} = \left[\frac{\partial z}{\partial \tau} \right]_{c_i} \quad \mu_{x_i} \equiv \left[\frac{\partial z}{\partial \tau} \right]_{x_i} \quad (10)$$

The adjusted velocity μ can be related to the usual velocity u as follows:

$$u = \frac{u_o}{1 + \bar{C}/C\mu} \quad , \quad (11)$$

Or

$$\mu = \frac{\bar{C}}{C(u_o - u)} \quad . \quad (12)$$

The assumptions of the Interference Theory are the following: 1. Uniform packing and plug flow; 2. negligible heat effects; 3. stoichiometric ion exchange; 4. no mass transfer effects; 5. constant separation factors; and 6. coherence. Coherence means that the changes in concentrations of different species occur at the same time. Therefore,

$$\mu_{x_i} = \mu_{x_j} \quad (13)$$

Since the stationary and mobile phases are locally in equilibrium,

$$\mu = \mu_{x_i} = \mu_{y_i} \quad (14)$$

The equation of continuity of any species i in a fixed bed is given as follows:

$$\frac{\partial}{\partial t}(\bar{C}_i + C_i) = -u_o \left[\frac{\partial C_i}{\partial z} \right]_t \quad (i = 1, 2, \dots, n) \quad (15)$$

the above equation can be written in terms of the dimensionless concentrations x_i , y_i and the adjusted time τ :

$$\left[\frac{\partial y_i}{\partial \tau} \right]_x + \left[\frac{\partial x_i}{\partial z} \right]_r = 0 \quad (i = 1, 2, \dots, n) \quad (16)$$

From the above continuity equation and the cyclic relation,

$$\left(\frac{\partial z}{\partial t} \right)_{C_i} \left(\frac{\partial C_i}{\partial z} \right)_t \left(\frac{\partial t}{\partial C_i} \right)_z = -1 \quad (17)$$

it can be shown that

$$\mu_{x_i} = \left(\frac{\partial z}{\partial \tau} \right)_{x_i} = \left(\frac{\partial x_i}{\partial y_i} \right)_z \quad (18)$$

$$\mu_{y_i} = \left(\frac{\partial z}{\partial \tau} \right)_{y_i} = \left(\frac{\partial x_i}{\partial y_i} \right)_{\tau} \quad (19)$$

and

$$dy_i = \frac{1}{\mu_{x_i}} dx_i = \lambda_i dx_i \quad (20)$$

where

$$\lambda_i \equiv 1/\mu_{x_i} \quad (21)$$

The assumption of coherence requires that all the λ_i 's are equal. Therefore,

$$dy_i = \lambda dx_i \quad (22)$$

From the above equation together with the assumptions of constant separation factors and stoichiometric exchange one can show that¹⁴

$$\sum_i \frac{x_i}{\alpha_{1i} - h} = 0 \quad \text{or} \quad \sum_i \frac{y_i}{\alpha_{i1} - 1/h} = 0 \quad (23)$$

Where $h = \mu y_1/x_1$. These equations relate or transform a set of compositions (x_i, y_i) to a set of h values. These are called the h -transform equations. For a system with n components, it is clear from Eq. (23) that there can be at most $(n-1)$ h values, which are bounded by the separation factors and therefore can be easily solved from one of the h -transform equations.

$$1 \leq h_1 \leq \alpha_{12} \leq h_2 \leq \alpha_{13} \dots \leq h_{n-1} \leq \alpha_{1n} \quad (24)$$

The compositions of species k can be readily calculated from the following inverse transformation:

$$x_k = \frac{\prod_{i=1}^{n-1} (\alpha_{1k} - h_i)}{\prod_{j \neq k} (\alpha_{1k} - \alpha_{1j})}, \quad y_k = \frac{\prod_{i=1}^{n-1} (1/\alpha_{1k} - 1/h_i)}{\prod_{j \neq k} (1/\alpha_{1k} - 1/\alpha_{1j})} \quad (25)$$

In this h -transform method, one can obtain the compositions without solving a set of coupled partial differential equations. In addition, because of the orthogonal nature of the h -space, only one h value can change across a boundary (or wave), whereas concentrations of all species may change across the boundary. This property made the construction of column profiles very simple, as shown in the step change case discussed below.

1. COLUMN RESPONSE TO A SINGLE STEP CHANGE

For a system with n species, a single step change in influent composition will generate at most $(n-1)$ transient waves. Therefore, at a given time, there could be n plateaus in the column profile. These waves propagate through the column at different speeds. The first plateau is the plateau near the column inlet. The composition of the first plateau is in equilibrium with the new influent. The composition of the n th plateau, which is near the column exit, is in equilibrium with the presaturant. Given the influent and presaturant compositions, one can easily solve the h'_i values corresponding to the influent composition and the h''_i values corresponding to the presaturant. Since only one h value can change across a coherent wave, the h values for the intermediate plateaus can be easily determined as follows:

Zone	h -Values
1	$h'_1, h'_2, \dots, h'_{n-1}$
2	$h''_1, h'_2, \dots, h'_{n-1}$
k	$h''_1, h''_2, \dots, h''_{k-1}, h'_k, \dots, h'_{n-1}$
n	$h''_1, h''_2, \dots, h''_{n-1}$

Once the h -values for each plateau zone are found, the corresponding plateau compositions can be easily calculated from the inverse transform, Eq. (25). In addition, the adjusted composition velocity can be calculated from the h values and α 's. For the k th wave, the adjusted upstream wave velocity μ'_k is³

$$\mu'_k = h_k'^2 P_k \quad (26)$$

$$\text{where } P_k \equiv \prod_{i=1}^{k-1} h_i'' \prod_{i=k+1}^{n-1} h_i' \prod_{i=1}^n \alpha_{i1} \quad (27)$$

The adjusted downstream wave velocity μ''_k is

$$\mu''_k = h_k''^2 P_k \quad (28)$$

If $\mu_k'' > \mu_k'$, the k th wave is diffuse. If $\mu_k' < \mu_k''$, the k th wave is sharp and its velocity $\mu_{\Delta k}$ is

$$\mu_{\Delta k} = (\mu_k' \mu_k'')^{\frac{1}{2}} \quad (29)$$

2. COLUMN RESPONSE TO MULTIPLE STEP CHANGES

A single step change can generate at most $(n-1)$ coherent waves which propagate through the column. A successive step change can generate another set of coherent waves. The faster waves in the second step change can catch up with the slower waves generated in the first step change. When two waves meet, the interference will result in enrichment of more preferred species in the upstream zone and less preferred species in the downstream zone. As mentioned before, each wave corresponds to a change in one h value. Let the index of changing h value for the wave generated in the first step change be j and that for the wave generated in the second step change be k . If $j=k$, the interference will result in a single wave. This case is called "merge". If $j \neq k$, the interference will result in two new waves and a new zone forms between the two waves. This case is called "cross-over". All the other h values remain the same as before the interference. The velocities of the new waves will change as a result of the interference. It has been shown that a faster wave decelerates as it crosses over a slower *sharp* wave, but accelerates as it crosses over a slower *diffuse* wave. On the other hand, a slower wave accelerates as it crosses over a faster *sharp* wave, but decelerates as it crosses over a faster *diffuse* wave³.

Displacement chromatography is a typical case involving multiple step changes. A column is presaturated with the least preferred species. A feed containing multiple species is then fed into the column. Solution containing the most preferred species is then used to displace the adsorbed solutes. Finally, the column is regenerated with solution containing the least preferred species. If the column is long enough for a given feed size, a "displacement train", which consists of zones containing pure species, will be formed. In the displacement train, more preferred species occupy the upstream regions whereas less preferred species occupy the downstream regions. In the fully developed stage, all the boundaries advance at the same speed.

Elution chromatography for concentrated systems is another typical case involving multiple step changes. A column is presaturated with species k . A feed is then injected into the column. Finally, solution containing only species k is used to elute and at the same time regenerate the column. Detailed column dynamic profiles for concentrated systems with one single step change and multiple step changes including elution and displacement are reported in the RESULTS AND DISCUSSION section.

III. COMPUTER SIMULATION SCHEMES

A computer program in FORTRAN 77 has been developed to simulate the column dynamics. The program displays numerically and graphically the column profiles at various times and effluent histories of all the species. The computation of column dynamics is carried out by integrating the equation $dz = u dt$ for each wave in the column. The program algorithm is summarized in a flow chart (Fig. 1) and explained below.

1. Read in separation factors, flow rates and compositions of presaturant and influent, integration time and step size, column dimensions, and column capacity.
2. Print the input data and plot the axis of time-distance diagram.
3. Calculate the H-roots of presaturant.
4. Set $t=0$
5. Calculate the H-roots of the i -th step change. For this step change, a set of waves are generated. Identify new waves generated and assign new indices to all the waves.
6. Identify the diffuse waves and break each diffuse wave into a large number (usually 100 or more) of sharp waves.
7. Calculate the velocity of each new wave.
8. Identify the positions of all the waves. For old waves, the positions remains unchanged; For new waves, the position are at the inlet ($z=0$).
9. Calculate and plot the wave positions at all waves at $t=t + \Delta t$. The new locations are found from $z_{\text{new}} = z_{\text{old}} + u\Delta t$.
10. Check interference. If two waves meet, check whether they crossover or merge by comparing the h roots which are changing across these two waves. For the case of cross over, new h values are found for the new zone, and the new velocities are then calculated. For the case of merge, calculate the new velocity of the merged wave.
11. Calculate the column profiles at time t if required. Store the profile for later output.
12. Calculate the effluent history at time t if required. Store the data for later output.
13. Check whether the desired integration time has been reached. If not, continue. If yes, go to 14. Check whether there is a new step input at this time. If yes, go to step 5. If not go to step 9.
14. Print and/or plot column profiles if required.

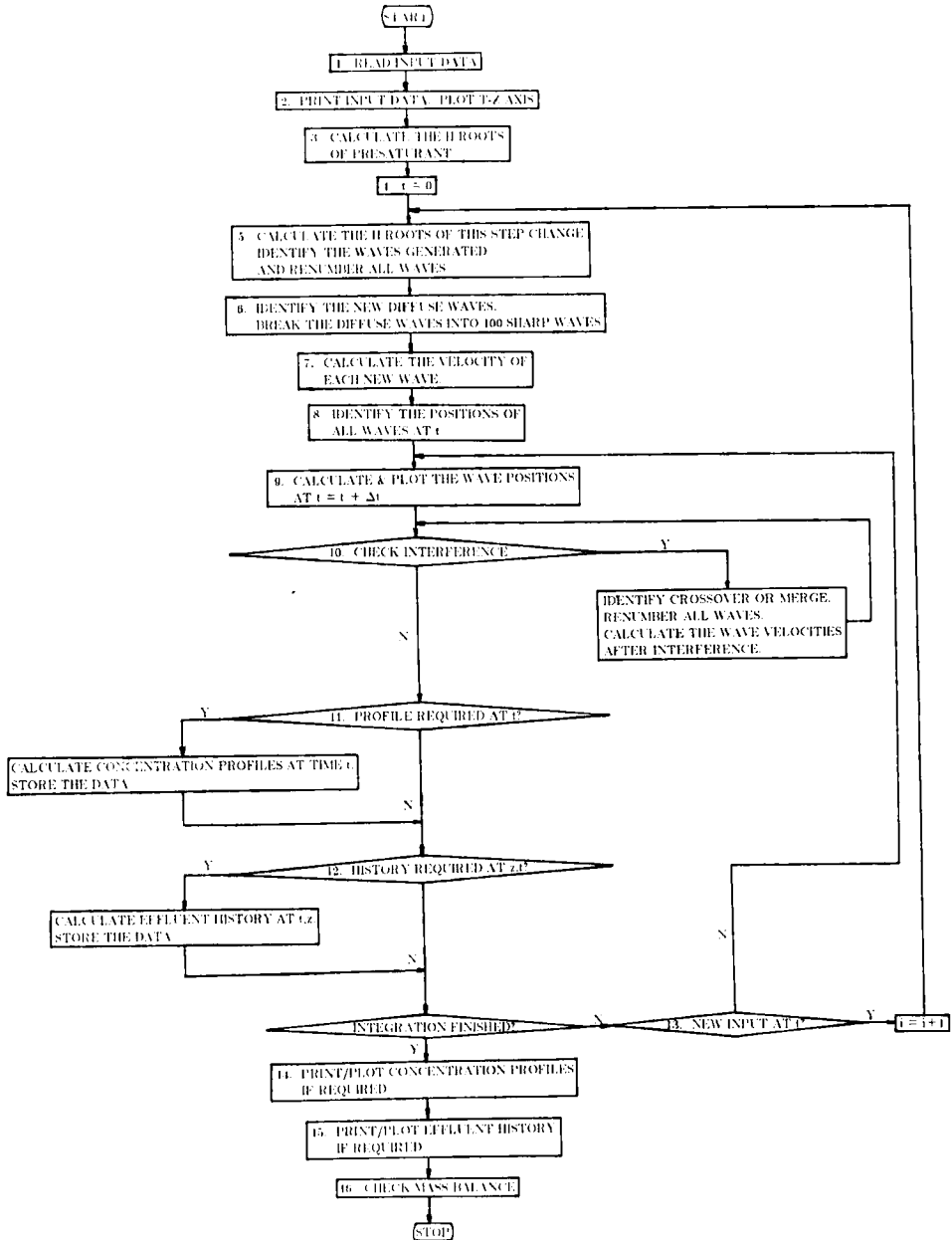


FIGURE 1.

Flow chart of the Computer Program

15. Print and/or plot effluent histories if required.
16. Check the mass balance by integrating the breakthrough curves. Print out the numerical results.

IBM 4341 computer has been used in all the simulations reported below. The operating system is VMSP (Virtual Machine System Product). The graphics package is GDDM (Graphical Display Data Manager).

IV. RESULTS AND DISCUSSION

1. DYNAMICS OF A SINGLE STEP CHANGE

Single step change is a basic element in chromatographic processes. Its dynamics are illustrated first. In this case, a column is presaturated uniformly, then a step change of composition in the influent is introduced. When a more preferred species displaces a less preferred species, there is a sharp wave traveling through the column (Fig. 2). At $T = 1.0$, Species 2 is totally displaced by Species 1. When a less preferred species displaces a more preferred species, there is a diffuse wave (Fig. 3). The diffuse wave spreads as it travels through the column. The larger the difference between the affinities of the two species, the more spread the diffuse wave. Notice that it takes a longer time period ($T \sim 2.0$) for Species 1 to be totally displaced by Species 2 (Fig 3).

Figures 4,5,6 show the column dynamics of three component systems. In the system shown in Fig. 4, because two more preferred species displacing a less preferred presaturant species there are two sharp waves traveling through the column. In the system shown in Fig. 5, the presaturant affinity is in between those of the two solutes. This system has one sharp wave and one diffuse wave. The system shown in Fig. 6 is the opposite of the system in Fig. 4. The presaturant is more preferred than the solutes. Two diffuse waves are formed because two less preferred species displace a more preferred species.

2. DYNAMICS OF DISPLACEMENT DEVELOPMENT

In displacement development, the column is presaturated with the least preferred species, then a pulse which contains solutes with higher affinities than the presaturant is introduced. The absorbed solutes are then displaced by a displacer containing the most preferred species. Finally, the column is regenerated with the presaturant. The simplest displacement system is a 4-component system, where Species 4 is the presaturant, Species 1 is the displacer, and Species 2 and 3 are the

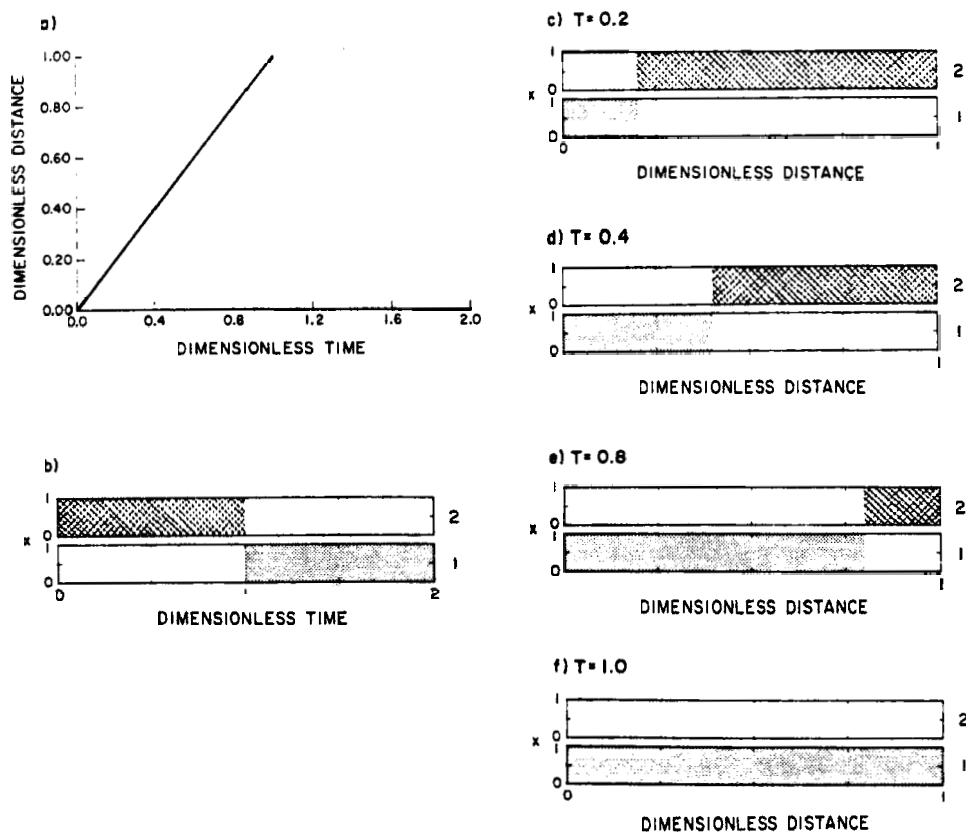


FIGURE 2.

Dynamics of Single Step Change ($1 \rightarrow 2$); Presaturant: $x_2 = 1.0$; Influent: $x_1 = 1.0$; Separation Factors: $\alpha_{11} = 1.0$, $\alpha_{12} = 2.0$; (a) Time-Distance Diagram; (b) Effluent History; Concentration profiles at (c) $T = 0.2$; (d) $T = 0.4$; (e) $T = 0.8$; (f) $T = 1.0$.

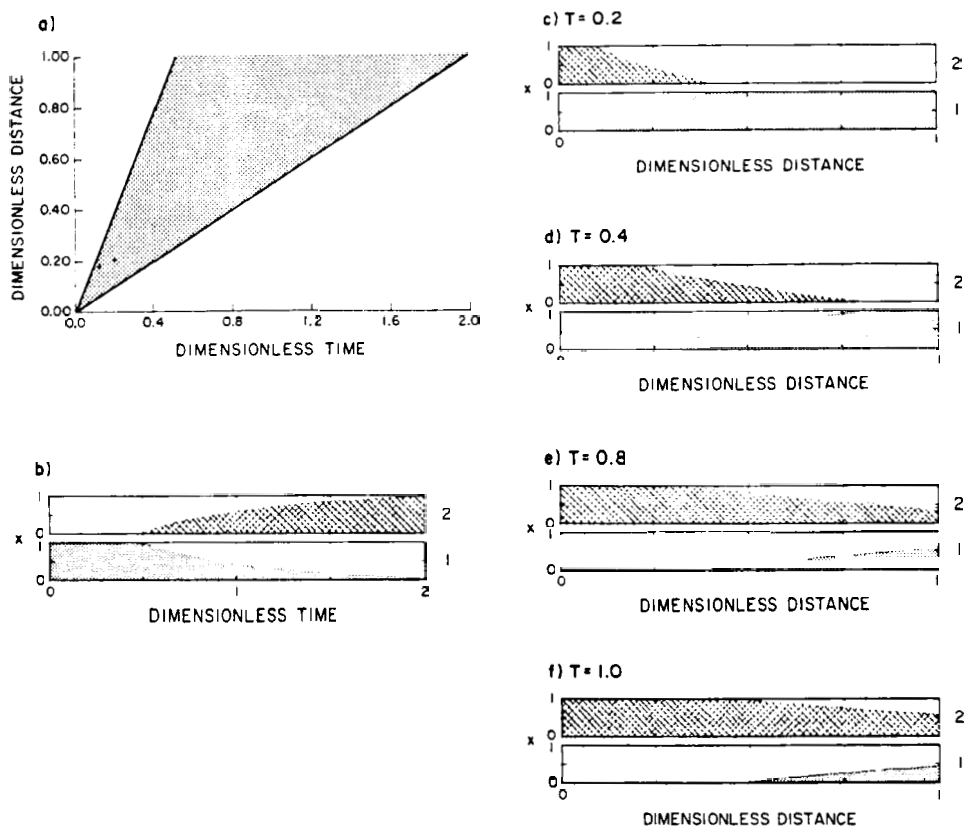


FIGURE 3.

Dynamics of Single Step Change ($2 \rightarrow 1$); Presaturant: $x_1 = 1.0$; Influent: $x_2 = 1.0$; Separation Factors: $\alpha_{11} = 1.0$, $\alpha_{12} = 2.0$; (a) Time-Distance Diagram; (b) Effluent History; Concentration profiles at (c) $T = 0.2$; (d) $T = 0.4$; (e) $T = 0.8$; (f) $T = 1.0$.

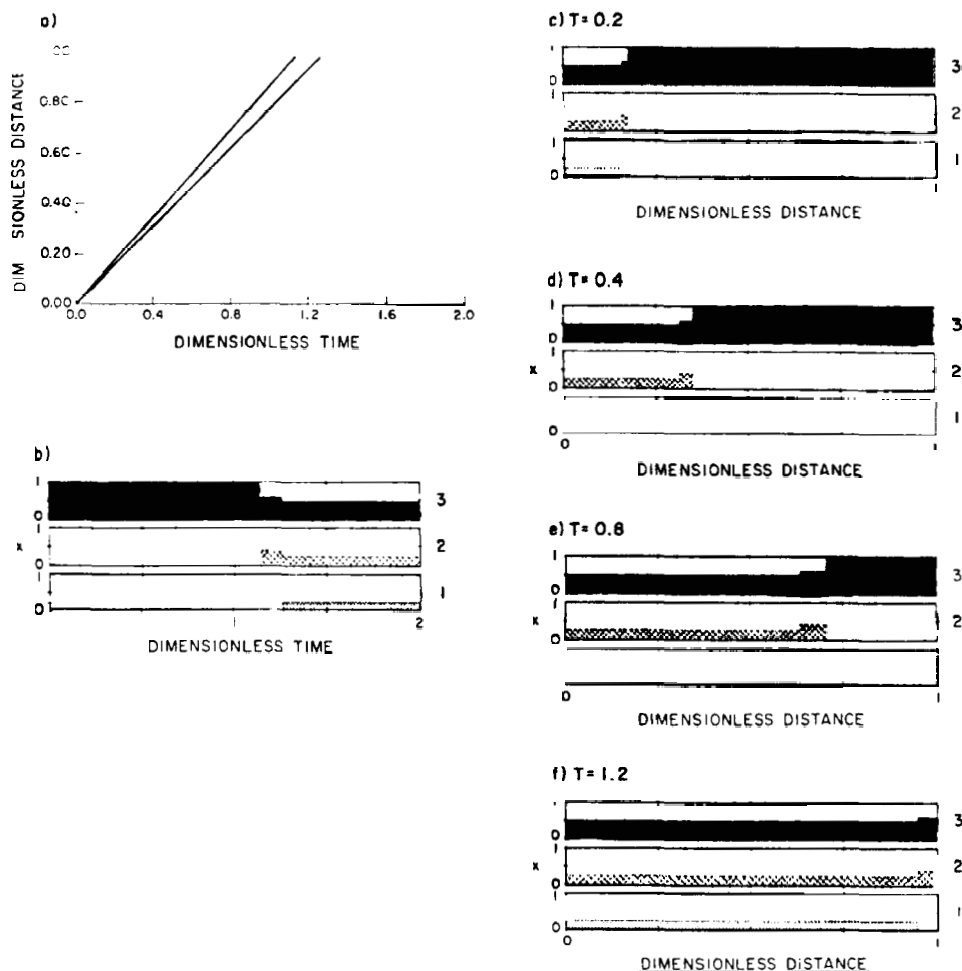


FIGURE 4.

Dynamics of Single Step Change (1,2,3 \rightarrow 3); Presaturant: $x_3 = 1.0$; Influent: $x_1 = 0.25$, $x_2 = 0.25$, $x_3 = 0.50$; Separation factors: $\alpha_{11} = 1.0$; $\alpha_{12} = 1.2$; $\alpha_{13} = 1.5$; (a) Time-Distance Diagram; (b) Effluent History; Concentration profiles at (c) $T = 0.2$; (d) $T = 0.4$; (e) $T = 0.8$; (f) $T = 1.2$.

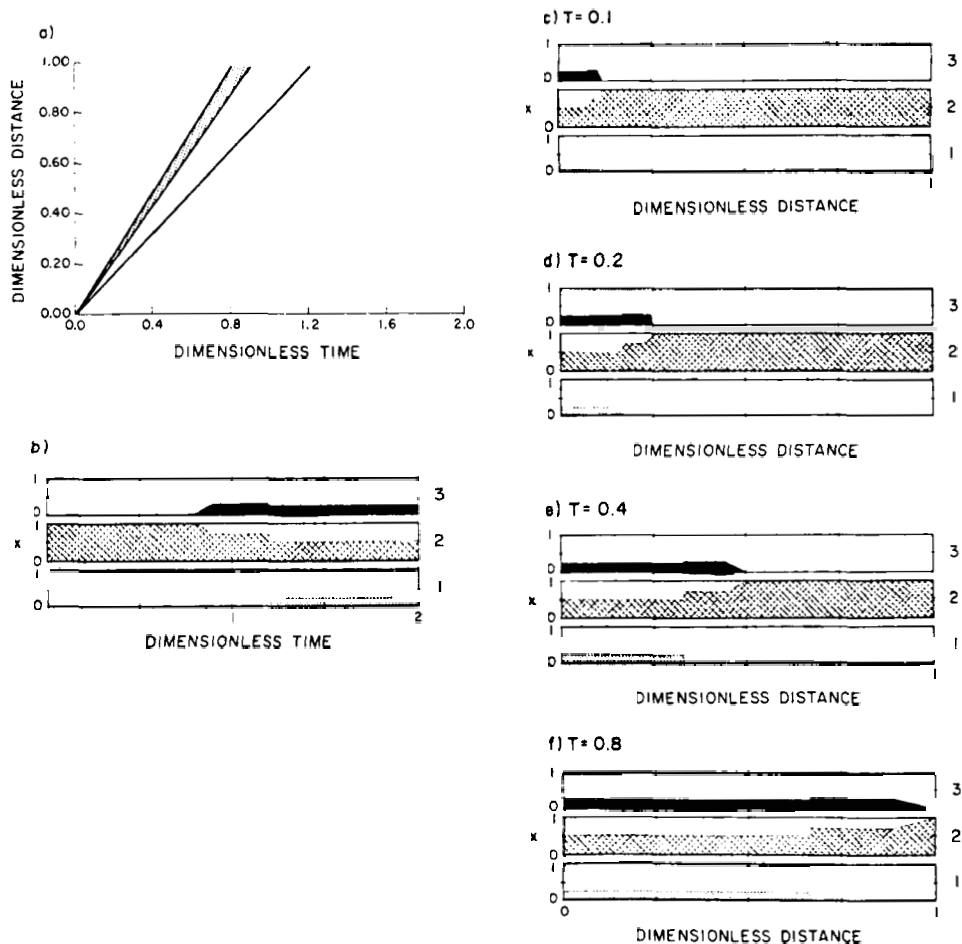


FIGURE 5.

Dynamics of Single Step Change (1,2,3 \rightarrow 2); Presaturant: $x_2 = 1.0$; Influent: $x_1 = 0.25$, $x_2 = 0.50$, $x_3 = 0.25$; Separation Factors: $\alpha_{11} = 1.0$, $\alpha_{12} = 1.2$, $\alpha_{13} = 1.5$; (a) Time-Distance Diagram; (b) Effluent History; Concentration profiles at (c) $T = 0.1$; (d) $T = 0.2$; (e) $T = 0.4$; (f) $T = 0.8$.

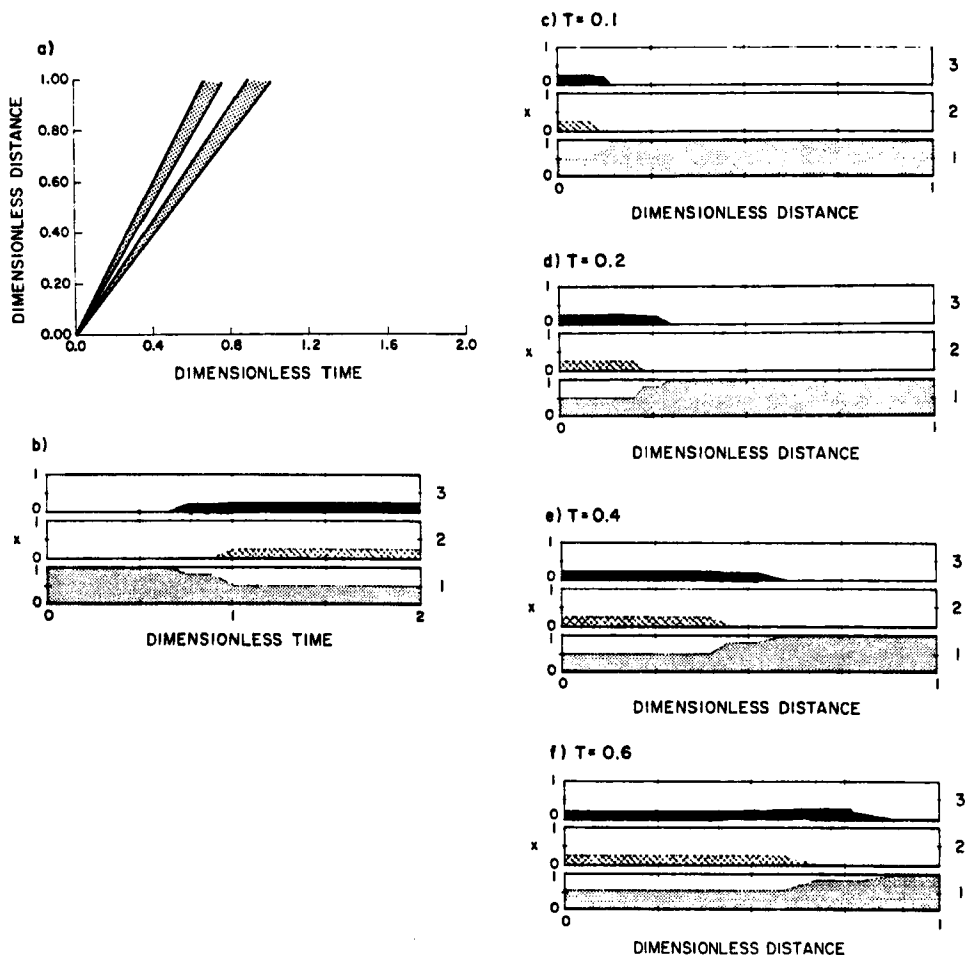


FIGURE 6.

Dynamics of Single Step Change ($1,2,3 \rightarrow 1$); Presaturant: $x_1 = 1.0$; Influent: $x_1 = 0.50$, $x_2 = 0.25$, $x_3 = 0.25$; Separation factors: $\alpha_{11} = 1.0$, $\alpha_{12} = 1.2$, $\alpha_{13} = 1.5$; (a) Time-Distance Diagram; (b) Effluent History; Concentration profiles at (c) $T = 0.1$; (d) $T = 0.2$; (e) $T = 0.4$; (f) $T = 0.6$.

solutes. The dynamics of the system is shown in Fig. 7. The regeneration step is similar to the single step change case shown in Fig. 3. Since the regeneration always generates a diffuse wave, the closer of the presaturant and displacer affinities, the shorter the total cycle time.

In displacement development, all the waves are sharp and bounded in a band by two sharp waves with an adjusted velocity $\mu = 1$. If the column is long enough, the interference of the waves eventually results in pure solute bands moving with the same adjusted velocity $\mu = 1$.

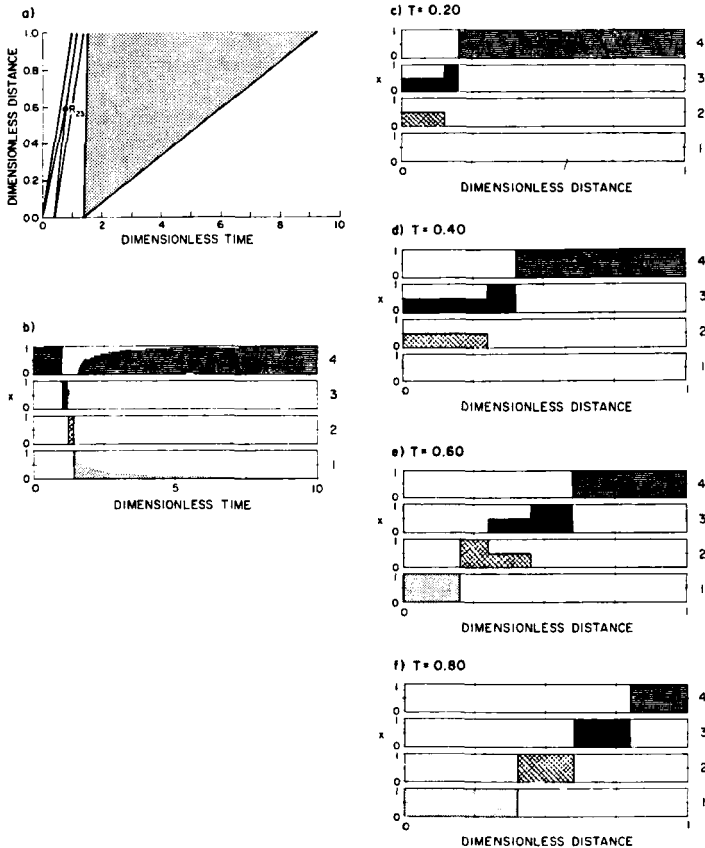


FIGURE 7.

Dynamics of Displacement ($1 \rightarrow 2,3 \rightarrow 4$); Presaturant: $x_4 = 1.0$; Feed: $\Delta T = 0.4$, $x_2 = 0.5$, $x_3 = 0.5$; Displacer: $T = 1.4$; $x_1 = 1.0$; Separation factors: $\alpha_{11} = 1.0$, $\alpha_{12} = 2.0$, $\alpha_{13} = 4.0$, $\alpha_{14} = 8.0$; (a) Time-Distance Diagram; (b) Effluent History; Concentration profiles at (c) $T = 0.2$; (d) $T = 0.4$; (e) $T = 0.6$; (f) $T = 0.8$.

This is called the fully developed displacement train, in which the more preferred species concentrate upstream from the less preferred species. Mass transfer effects, if important, will cause the solute bands to spread and overlap as they migrate through the column¹².

In the time-distance diagram, point R_{23} is called the resolution point, where species 2 and 3 are completely separated. In order to use the column more efficiently we can increase the feed size so that the resolution point occurs at about $Z^* = 1.0$. Therefore, computer simulations and the time-distance diagram can be used in finding the largest feed size for the desired separation.

Fig. 8 shows the dynamics of a five-component displacement process. Resolution points R_{23} and R_{34} indicate the separations of Species 2 and 3 and Species 3 and 4 respectively. We can further optimize the column loading by making the desired separation point R_{34} occur at about $Z^* = 1$.

3. DYNAMICS OF SELECTIVE DISPLACEMENT

In selective displacement, the presaturant and displacer are the same as in the displacement process but an additional displacer Species 3 is used to ensure the total separation of Species 2 and 4. Selective displacement eventually develops into the same final pattern as in displacement development. This is shown in Fig. 9. The regeneration for selective displacement is the same as for displacement.

The cycle time of the selective displacement is longer than that for the displacement. The reason is that in selective displacement part of the column is used for separation of Species 2 and 3. Species 3 has to displace Species 2 in order to form a pure band between those of Species 2 and 4.

4. DYNAMICS OF ELUTION

In elution the presaturant and displacer are the same. Figures 10,11,12 show the dynamics of three component systems for separating two solutes. In Fig. 10, the eluent is less preferred than the two solutes. The solute peaks spread as they travel through the columns. The effluent history has two peaks with a sharp left flank and a right diffuse flank. The flat tops of the peaks will eventually disappear upon migration if a longer column or a smaller feed is used³. In Fig. 11, the eluent affinity is in between the two solutes. The effluent history has one peak with a sharp left flank and a diffuse right flank and one peak with the opposite shape. In Fig. 12, the effluent history has two peaks with diffuse left flanks and sharp right flanks. The solute peaks within the column have an opposite shape. As the peaks migrate through the column, they did not spread as much as the peaks in Fig. 10.

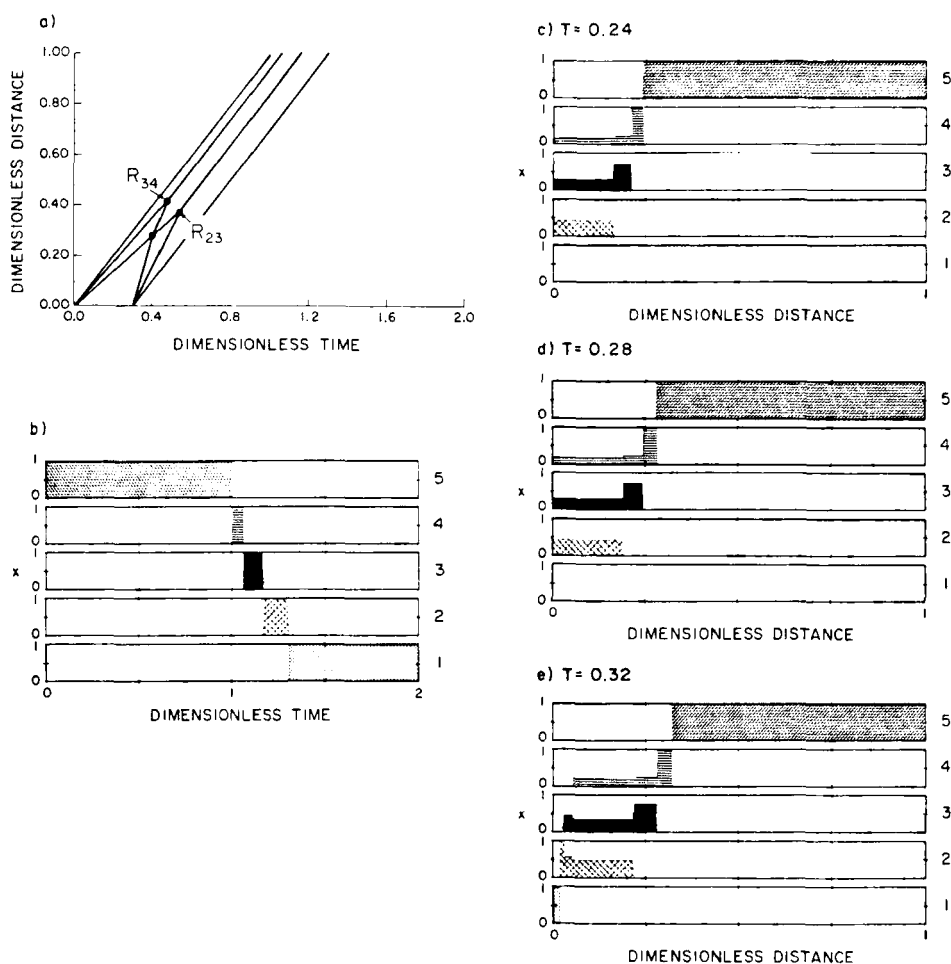


FIGURE 8.

Dynamics of Displacement ($1 \rightarrow 2,3,4 \rightarrow 5$); Presaturant: $x_5 = 1.0$; Displacer: $x_1 = 1.0$; Feed: $\Delta T = 0.3$; $x_2 = 0.33$; $x_3 = 0.2$; $x_4 = 0.47$; Separation Factors: $\alpha_{11} = 1.0$; $\alpha_{12} = 2.0$; $\alpha_{13} = 4.0$; $\alpha_{14} = 8$; $\alpha_{15} = 10$; (a) Time-Distance Diagram; (b) Effluent History; Concentration profiles at (c) $T = 0.24$; (d) $T = 0.28$; (e) $T = 0.32$; (f) $T = 0.38$; (g) $T = 0.42$; (h) $T = 0.44$; (i) $T = 0.50$; (j) $T = 0.55$; (k) $T = 0.70$.

(Continued)

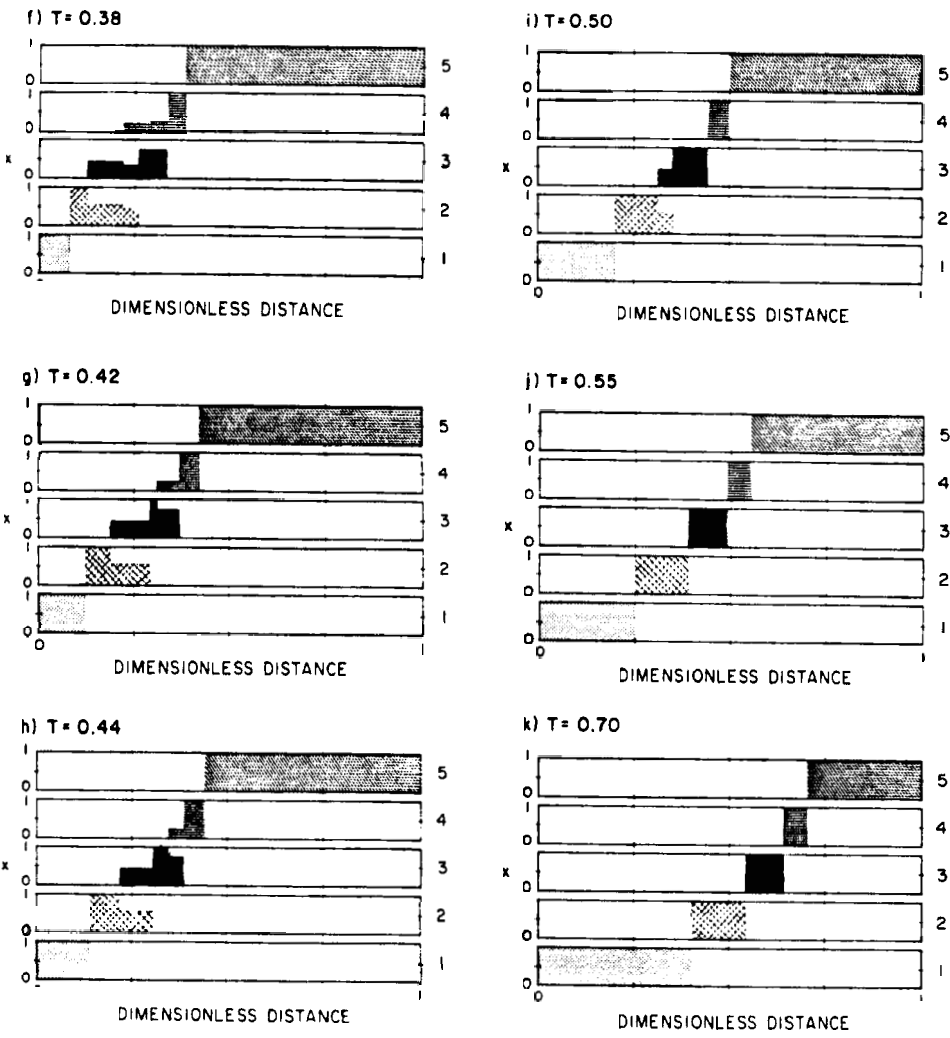


FIGURE 8 (CONTINUED)

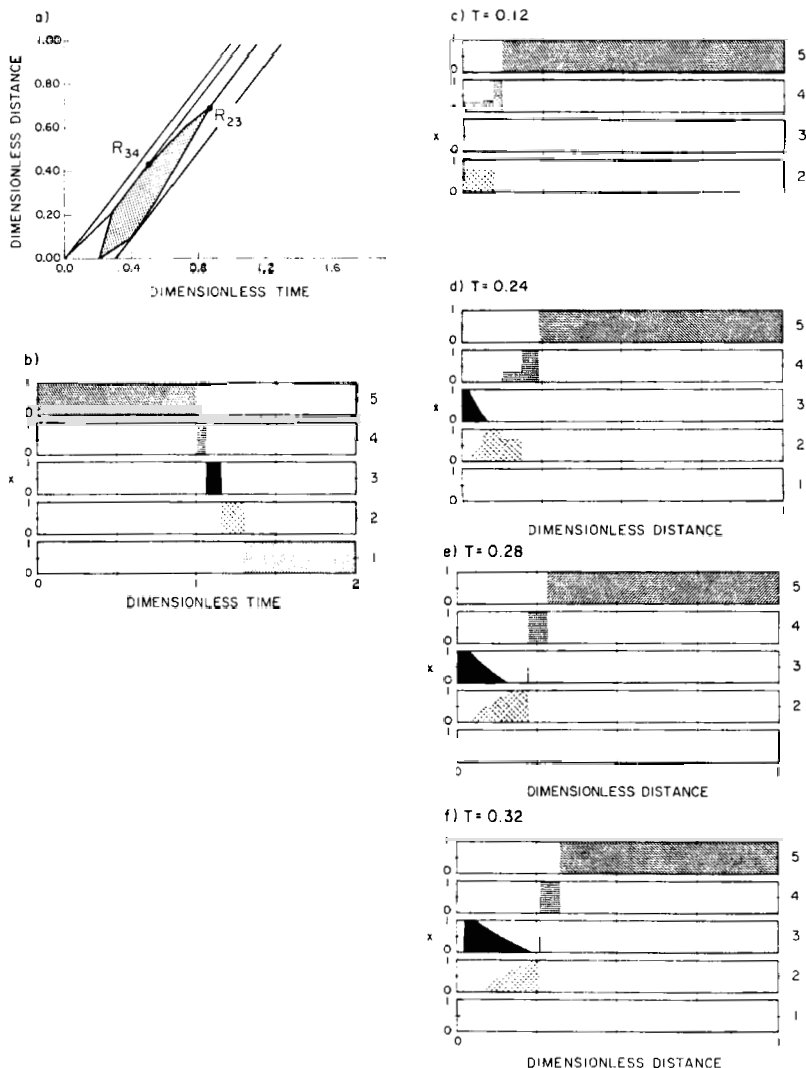


FIGURE 9.

Dynamics of Selective Displacement ($1 \rightarrow 3 \rightarrow 2, 4 \rightarrow 5$); Presaturant: $x_5 = 1.0$; Feed: $\Delta T_1 = 0.2$; $x_2 = 0.70$; $x_4 = 0.30$; Displacer 1: $\Delta T_2 = 0.1$; $x_3 = 1.0$; Displacer 2: $x_1 = 1.0$; Separation Factors: the same as in Figure 8; (a) Time-Distance Diagram; (b) Effluent History; Concentration profiles at (c) $T = 0.12$; (d) $T = 0.24$; (e) $T = 0.28$; (f) $T = 0.32$; (g) $T = 0.38$; (h) $T = 0.42$; (i) $T = 0.44$; (j) $T = 0.50$; (k) $T = 0.55$; (l) $T = 0.65$; (m) $T = 0.80$; (n) $T = 0.90$.

(Continued)

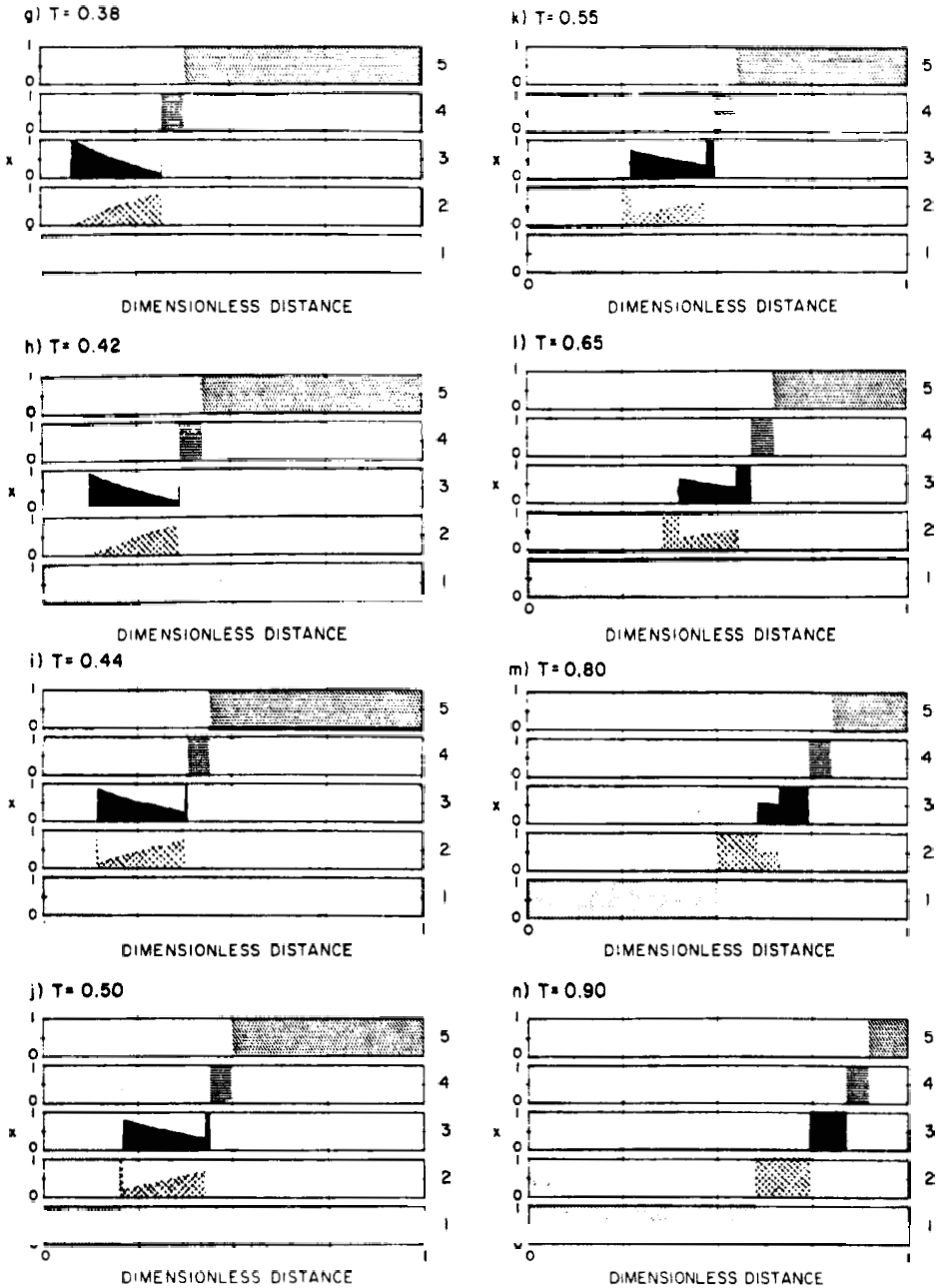


FIGURE 9 (CONTINUED)

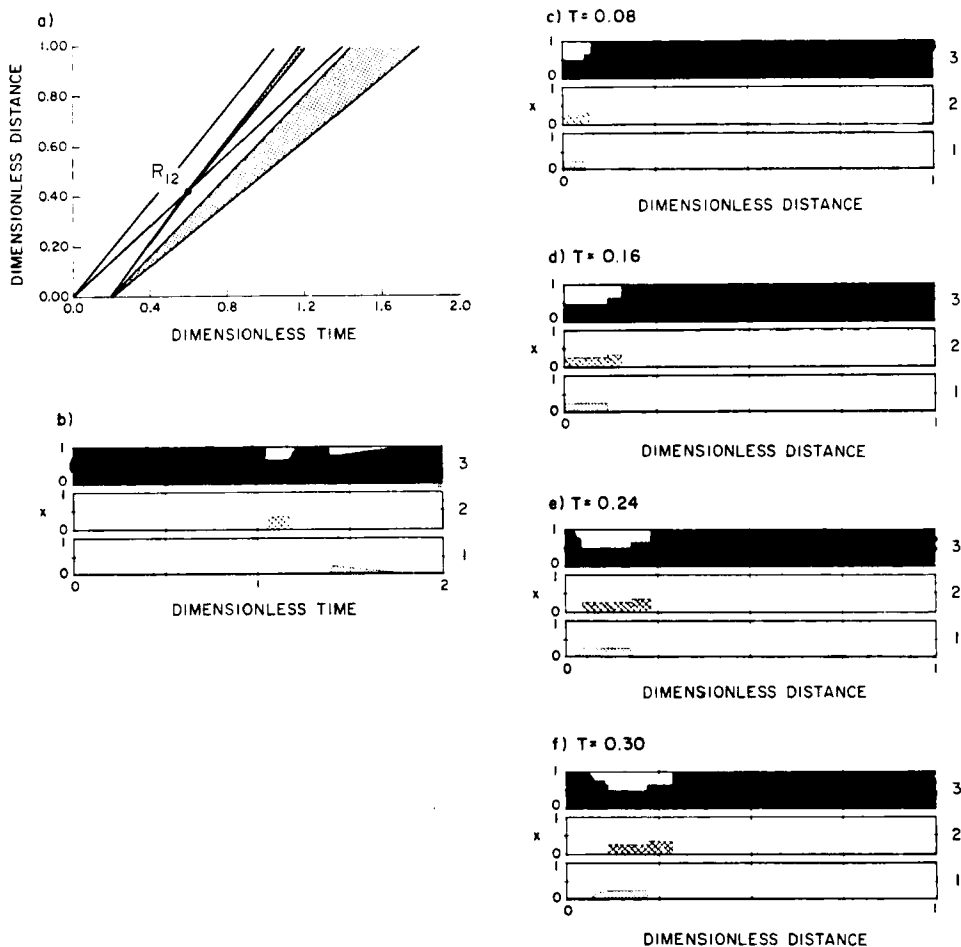


FIGURE 10.

Dynamics of Elution ($3 \rightarrow 1, 2, 3 \rightarrow 3$); Eluent: $x_3 = 1.0$; Feed: $\Delta T = 0.20$; $x_1 = 0.25$, $x_2 = 0.25$; $x_3 = 0.50$; Separation factors: $\alpha_{11} = 1.0$; $\alpha_{12} = 1.5$; $\alpha_{13} = 1.6$; (a) Time-Distance Diagram; (b) Effluent History; Concentration profiles at (c) $T = 0.08$; (d) $T = 0.16$; (e) $T = 0.24$; (f) $T = 0.30$; (g) $T = 0.45$; (h) $T = 0.60$; (i) $T = 0.75$; (j) $T = 1.00$.

(Continued)

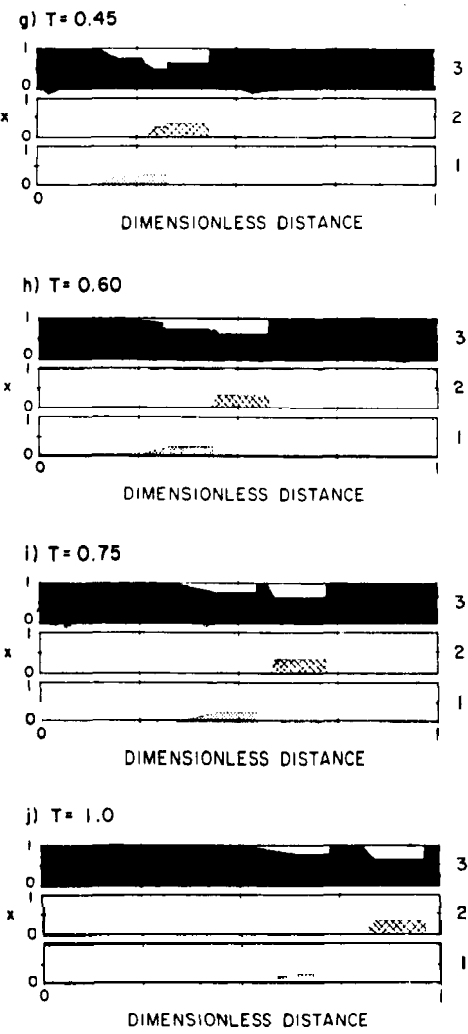


FIGURE 10 (CONTINUED)

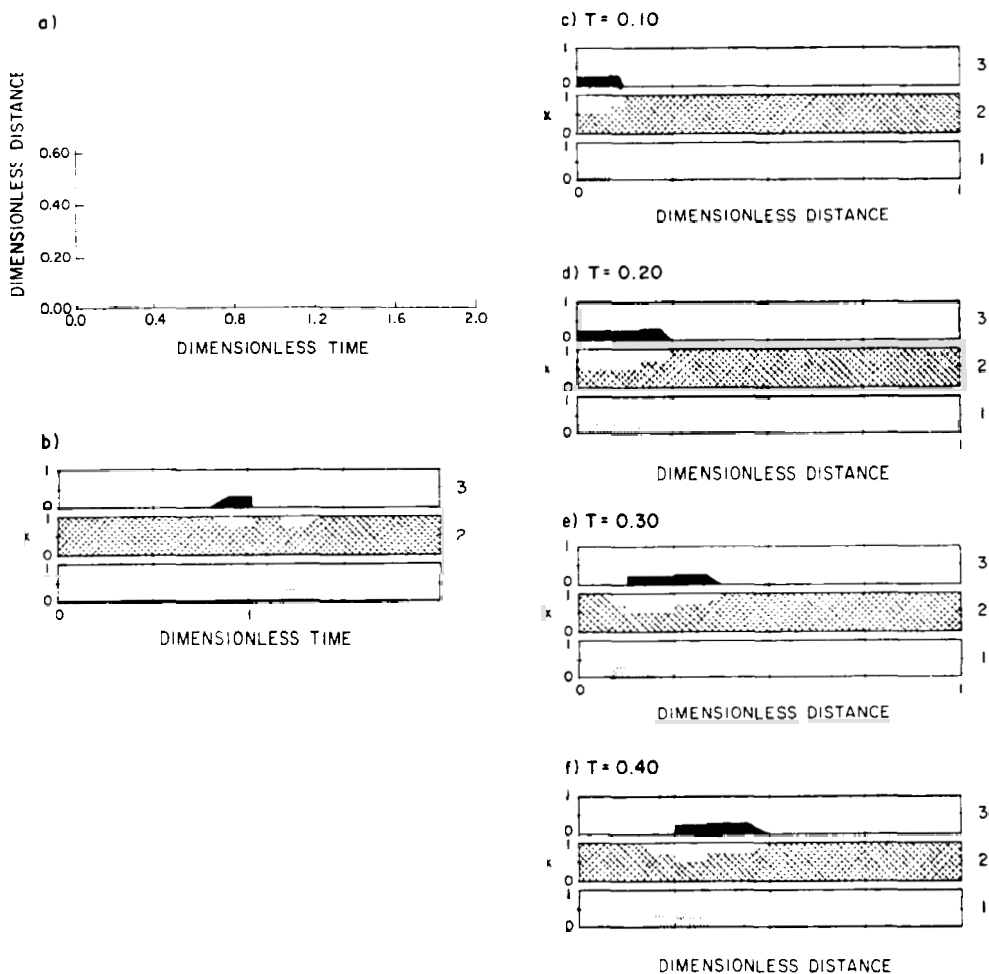


FIGURE 11.

Dynamics of Elution ($2 \rightarrow 1,2,3 \rightarrow 2$); Eluent: $x_2 = 1.0$; Feed: $\Delta T = 0.20$; $x_1 = 0.25$; $x_2 = 0.50$; $x_3 = 0.25$; Separation factors: $\alpha_{11} = 1.0$; $\alpha_{12} = 1.2$; $\alpha_{13} = 1.5$; (a) Time-Distance Diagram; (b) Effluent History; Concentration profiles at (c) $T = 0.10$; (d) $T = 0.20$; (e) $T = 0.30$; (f) $T = 0.40$; (g) $T = 0.50$; (h) $T = 0.60$; (i) $T = 0.70$; (j) $T = 0.80$; (k) $T = 0.90$; (l) $T = 1.0$; (m) $T = 1.10$; (n) $T = 1.20$.

(Continued)

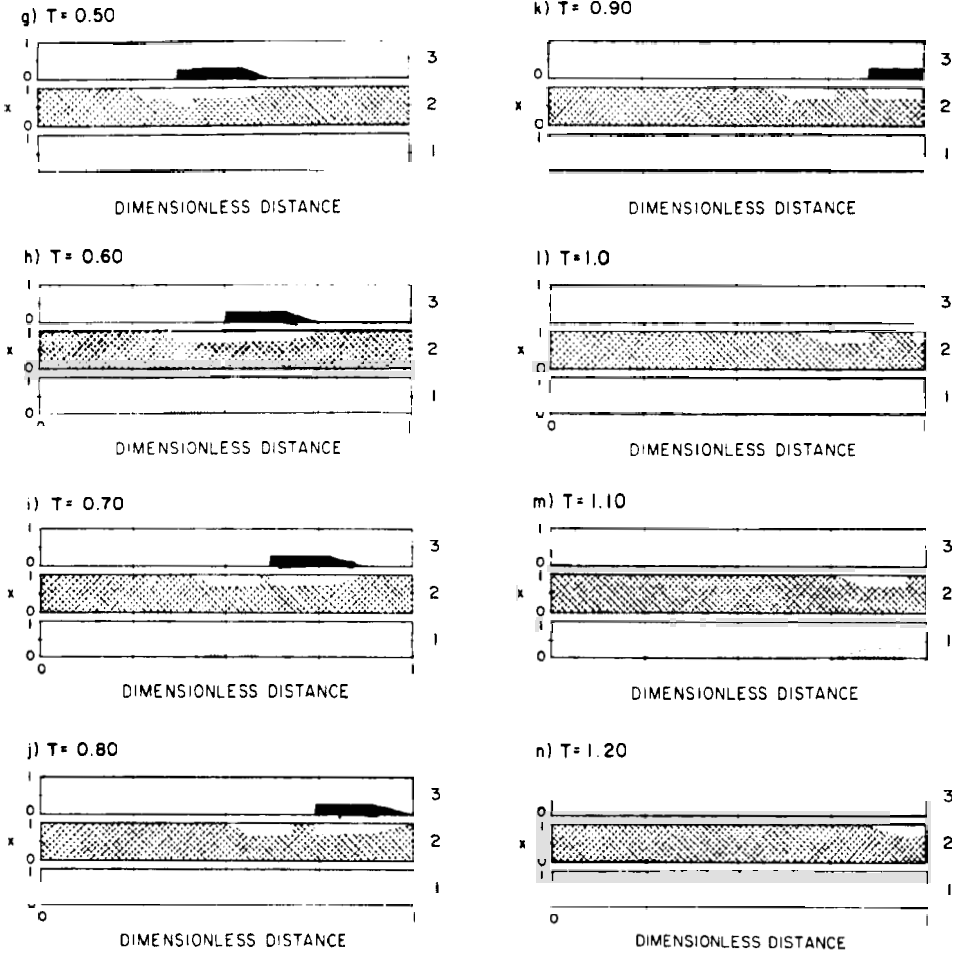


FIGURE 11 (CONTINUED)

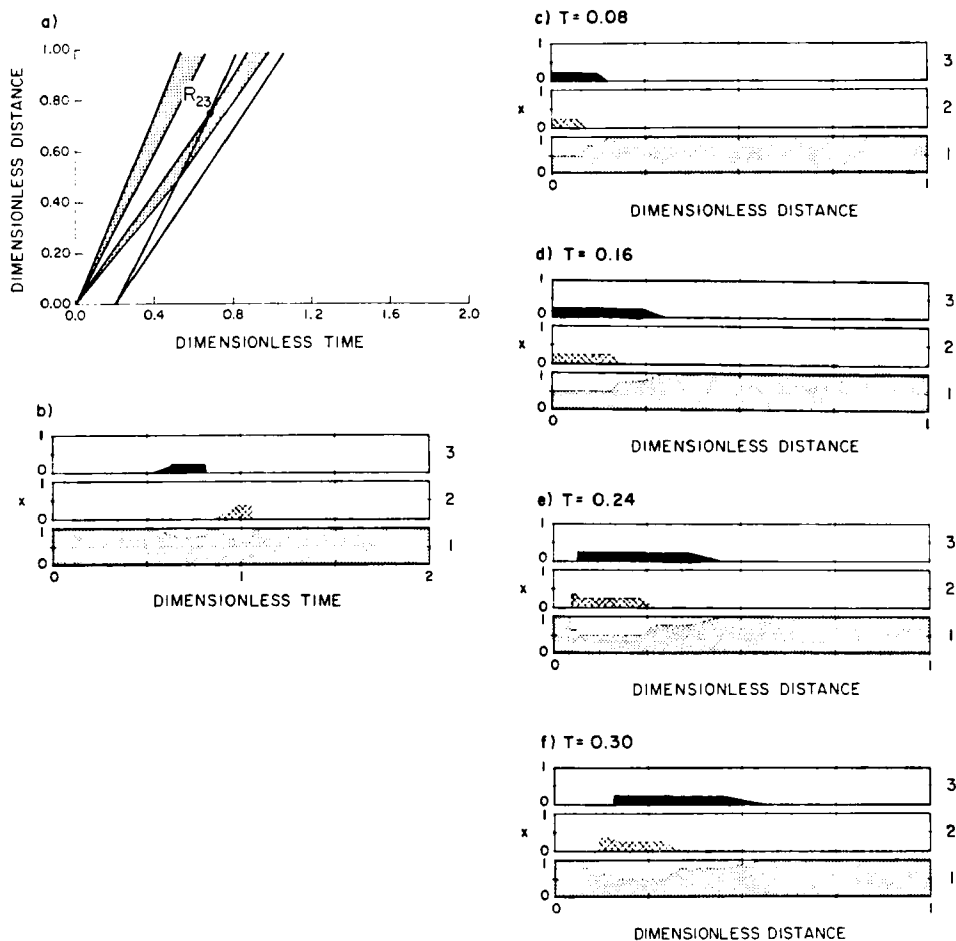


FIGURE 12.

Dynamics of Elution ($1 \rightarrow 1,2,3 \rightarrow 1$) Eluent: $x_1 = 1.0$; Feed: $\Delta T = 0.2$; $x_1 = 0.5$; $x_2 = 0.25$; $x_3 = 0.25$; Separation Factors: $\alpha_{21} = 0.8$; $\alpha_{22} = 1.0$; $\alpha_{23} = 1.5$; (a) Time-Distance Diagram; (b) Effluent History; Concentration profiles at (c) $T = 0.08$; (d) $T = 0.16$; (e) $T = 0.24$; (f) $T = 0.30$; (g) $T = 0.45$; (h) $T = 0.60$; (i) $T = 0.75$; (j) $T = 1.00$.

(Continued)

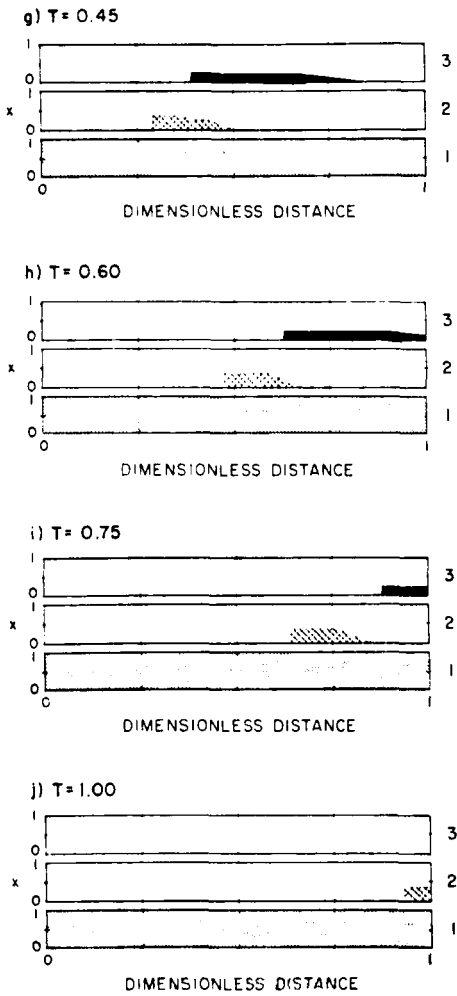


FIGURE 12 (CONTINUED)

It is clear from the elution dynamics that the concept of plate height can not be applied to concentrated systems. The eluted peaks are not symmetric as in dilute systems with linear isotherms. The spread and distortion of the peaks depend on the relative affinities and concentrations of the competing species.

In the system shown in Fig. 12, Solute 2 and Solute 3 are totally separated at $T \sim 0.7$. This can be identified as the point R_{23} on the time-distance diagram in Fig. 12a. About 77% of the column is utilized for separation whereas the rest 13% of the column is wasted. We can increase the column utilization from 77% to 100% by increasing the feed loading from $\Delta T = 0.2$ to $\Delta T = 0.26$ as shown in Fig. 13. In this case, the two solute bands exit the column consecutively and the column is completely utilized for separation. It is evident from the time-distance diagram, Fig. 13a, that the resolution point R_{23} occurs

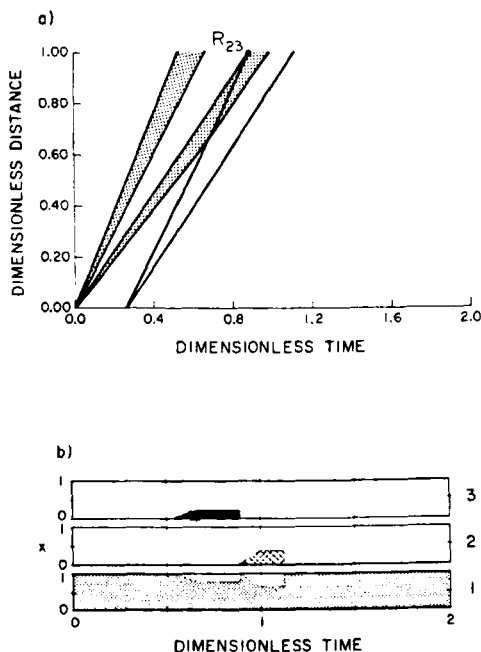


FIGURE 13.

Optimization of Feed Size. All the parameters are the same as those in Fig. 12 except $\Delta T = 0.26$.

near the exit of the column. If mass transfer effects are important, the maximum loading will be smaller than the predicted value based on this local equilibrium model.

It is evident from the effluent histories for these three cases that the affinity of the eluent affects the cycle time. The case shown in Fig. 12 has the shortest cycle time, $T = 1.06$, whereas the case shown in Fig. 10 has the longest cycle time; $T = 1.8$. In general, the greater the eluent affinity the shorter the cycle time. An example is shown in Fig. 14 to illustrate how the eluent affinity affects the cycle time, average product concentrations, maximum loading, and throughput. The throughput here is defined as the maximum feed loading, ΔT , divided by cycle time. In this example, the separation factor of Solute 1 against Solute 2 is 1.5. The feed contains 25% Solute 1, 25% Solute 2, and 50% eluent. The separation factor of Solute 1 against the eluent is varied from 0.7 to 2.0. It is clear from this figure that as the eluent affinity approaches that of a solute, the average product concentration of this solute is the

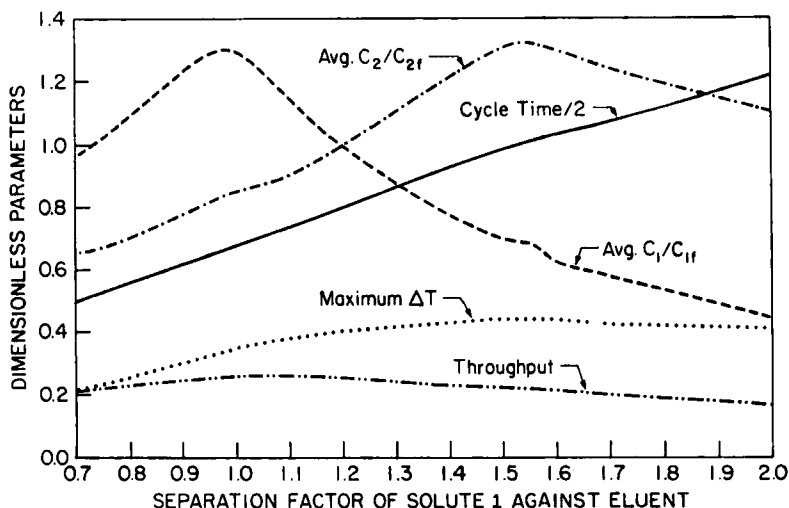


FIGURE 14.

The Effects of Eluent Affinity on Maximum Loading (.....), Half cycle Time (—), Average Product Concentrations (C_1/C_{1f} ----; C_2/C_{2f} - · - ·), and Throughput (· - ·). The separation factor of Solute 1 against Solute 2 is 1.5. The separation factor of Solute 1 against the eluent is varied from 0.7 to 2.0.

highest. As the eluent affinity increases, the cycle time decreases. Nevertheless, if the eluent has a much higher affinity than Solute 1, the column loading has to be reduced to obtain total separation of the two solutes. Consequently, throughput is the highest when the eluent affinity approaches that of Solute 1.

V. CONCLUSIONS

We have reported extensive computer simulations which illustrate the interference phenomena in multicomponent ion exchange columns. The following conclusions can be drawn:

1. A sharp wave is found when a more preferred species displaces a less preferred species. A diffuse boundary is found when a less preferred species displaces a more preferred species. The greater the difference in their affinities, the more diffuse the boundary.
2. In displacement chromatography, all the waves are sharp. If the feed loading is small enough, the interference of these waves results in a fully developed displacement train which consists of pure solute bands with more preferred species upstream and less preferred down stream. The closer the affinities of presaturant and displacer, the shorter the cycle time.
3. Selective displacement can achieve the same separation as displacement but a longer column is required.
4. In elution processes for concentration systems, the eluted peaks are not symmetric. If a solute has a higher affinity than the eluent, the eluted peak has a sharp left boundary and a diffuse right boundary in the effluent history. If a solute is less preferred than the eluent, the peak has the opposite shape. Throughput is the highest when the eluent affinity is the closest to the most preferred solute.
5. Computer simulations and time-distance diagrams can be used for optimizing column loadings and increasing the throughputs for elution and displacement processes.

ACKNOWLEDGEMENT:

This research has been supported by NSF (CPE 8412013) and the Whitaker Foundation. The helpful discussions and suggestions of Professors F. Regneir and P.C. Wankat are also acknowledged.

REFERENCES

1. J.C. Giddings, "Dynamics of Chromatography," Dekker, New York, 1965.
2. L.R. Snyder and J.J. Kirkland, "Introduction to Modern Liquid Chromatography," 2nd ed., Wiley, New York, 1979.
3. F. Helfferich and G. Klein, "Multicomponent Chromatography; Theory of Interference," Dekker, New York, 1970.
4. H.K. Rhee, R. Aris, and N.R. Amundson, *Phil. Trans. Roy. Soc. Lond. A*, 267 (1182), 419 (1970).
5. H.K. Rhee, in "Percolation Processes: Theory and Applications," Proceedings of the NATO Advanced Study Institute Programme, A.E. Rodrigues and D. Tondeur, ed., Sijthoff & Noordhoff, The Netherlands, 1981, p. 285.
6. H.K. Rhee, *AIChE J.*, 28 (3), 423, (1982).
7. D. Clifford, *Ind. Eng. Chem. Fundam.* 21, 141 (1982).
8. M. Bailly and D. Tondeur, *Chem. Eng. Sci.*, 37 (8), 1199 (1982).
9. N.-H.L. Wang, and S. Huang, *AIChE Symp. Ser. No. 230*, Vol. 79, 26 (1983).
10. N.-H.L. Wang and S. Huang, *Separation and Purification Methods*, 13 (1), 43 (1984).
11. C. Horvath, A. Nahum, and J.H. Frenz, *J. of Chromatography*, 218, 365 (1981).
12. C. Horvath, J. Frenz, and Z. El Rassi, *J. of Chromatography*, 255, 273 (1983).
13. M. Morbidelli, G. Storti, S. Carra, G. Niederjaufner, and A. Pontoglio, *Chem. Eng. Sci.*, 40 (7), 1155 (1985).
14. S. Huang, "Multicomponent Ion Exchange in Mixed Beds for Dialysate Regeneration," M.S. Thesis, Purdue University, 1983.